NANO LETTERS

Letter

pubs.acs.org/NanoLett

Harvesting Energy from Water Flow over Graphene?

Jun Yin, Zhuhua Zhang, Xuemei Li, Jianxin Zhou, and Wanlin Guo*

State Key Laboratory of Mechanics and Control of Mechanical Structures, Key Laboratory for Intelligent Nano Materials and Devices of the Ministry of Education, and Institute of Nanoscience, Nanjing University of Aeronautics and Astronautics, Nanjing 210016, China

Supporting Information

ABSTRACT: It is reported excitingly in a previous letter (*Nano Lett.* **2011**, *11*, 3123) that a small piece of graphene sheet about 30 × 16 μm^2 immersed in flowing water with 0.6 M hydrochloric acid can produce voltage ~20 mV. Here we find that no measurable voltage can be induced by the flow over mono-, bi- and trilayered graphene samples of ~1 × 1.5 cm^2 in size in the same solution once the electrodes on graphene are isolated from interacting with the solution, mainly because the H_3O^+ cations in the water adsorb onto graphene by strong covalent bonds as revealed by our first-principles calculations. When both the graphene and its metal electrodes are exposed to the solution as in the previous work, water flow over the graphene-electrode system can induce voltages from a few to over a hundred millivolts. In this situation, the graphene mainly behaves as a load connecting between the electrodes. Therefore, the harvested energy is not from the immersed carbon nanomaterials themselves in ionic water flow but dominated by the exposed electrodes.

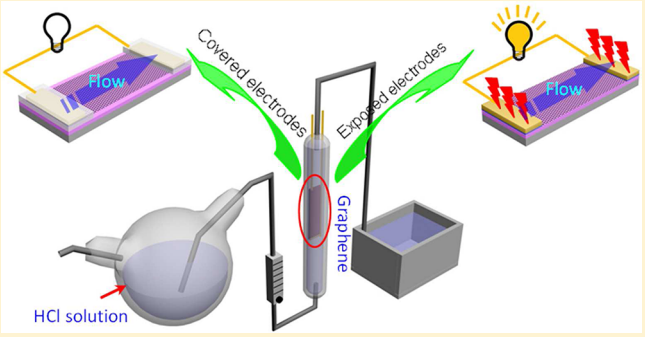

KEYWORDS: *Graphene, electrode, energy harvesting, water flow, ion adsorption*

Carbon nanomaterials, especially carbon nanotubes (CNTs) have been widely demonstrated to be capable of producing a voltage when being immersed in flowing water or polar liquids.[1−3] Single-walled CNTs mats packed between two metal electrodes spacing at 1 mm along the direction of the flow were first reported in 2003 to produce a voltage up to 10 mV in flowing HCl solution.[2] The induced voltage increases with flow velocity to a saturated value that depends sensitively on the ionic conductivity and polar nature of the liquids, but is about ten times smaller in multiwalled CNTs. In contrast, thin films of aligned multiwalled CNTs were later reported to induce voltage up to 20 mV even in pure water and higher in mild NaCl solution, but no details were mentioned about the electrodes.[3] Most recently, it was reported that semiconducting single-walled CNT film can produce voltage three times higher than metallic CNT film in flowing KCl solutions, but only at microvolt level.[4] Since the nanotube electron drag in flowing ionic liquids was proposed in 2001,[5] different mechanisms have been used to explain the flow-induced voltage in CNTs in independent experiments,[2,3,6−9] but none of them can provide satisfied explanation for all the observed phenomena. More excitingly, it was reported recently that a 30 × 16 μm^2 sized graphene surface surrounded by four patterned electrodes (Ti/Au, 3/30 nm, connected with gold wires by silver epoxy) can generate a peak voltage ~25 mV and power ~85 nW in flowing solution of 0.6 M HCl at ~1 cm/s, while only ~0.8 mV can be induced in aligned multiwalled CNTs in the same solution.[1] The flow-induced voltage in graphene was explained by a net drift velocity of Cl^- ions adsorbing/desorbing or hopping on graphene on the basis of a force-field molecular dynamics simulation, which showed no adsorbing or hoping of hydronium ions on the graphene. However, in all the mentioned literatures, the effect of the metal electrodes has never been addressed, and no mechanism study is found at the first-principles level. Here we show by extensive investigations that no flow-induced voltage can be measured in all our tests on mono-, bi- and trilayered graphene samples in a flowing water containing 0.6 M HCl at various velocities once no interaction between the electrodes and water is involved. Only when metallic electrodes are exposed to the water, the flow can induce voltage up to 150 mV, but the real-time electric signal is not stable and decays sharply to a few millivolts. Our first-principles simulations show that the Cl^- anions are repulsive to graphene, while H_3O^+ cations bind strongly through forming covalent bonds with the graphene sheet, and even stronger with CNTs, showing that the previous molecular dynamics results[1] can not provide correct physical picture in this kind of situations. The results highlight the important role of electrode−solution interaction in the creation of the flow-induced voltage for the first time and show convincingly that immersed graphene itself can not have flow-induced voltage generation.

Received: February 15, 2012
Revised: March 1, 2012
Published: March 1, 2012

   dx.doi.org/10.1021/nl300636g | *Nano Lett.* 2012, 12, 1736−1741

In this work, all the graphene samples were synthesized by low pressure chemical vapor deposition (CVD) on 25 μm thick copper foil (Alfa Aesar, item No.13382) using methane as precursor.[10,11] To transfer the graphene,[12−14] a thin layer of poly(methyl methacrylate) (PMMA) was spin-coated onto the graphene, and the underlying copper foil was then etched away by $FeCl_3$ solution. After washed by 0.6 M HCl and deionized water, the graphene was transferred onto the target substrates, namely the 300 nm SiO_2 on Si wafer or the polyester terephthalate (PET) depending on the size of the graphene sample (shown later), and the PMMA film was finally removed by acetone. The monolayer characteristic of the CVD graphene sample was confirmed by the Raman spectra and atomic force microscopy topography (Supporting Information, Figures S1 and S2).[15,16] The undetected D band of the Raman spectra suggested the high quality of our graphene sample. In addition to the monolayer graphene sample, we also fabricated bi- and trilayered graphene samples by means of layer-by-layer stacking. The intensity ratio of the G and 2D modes of the Raman spectra increases monotonically from 0.3 for monolayered graphene to 0.9 for trilayered graphene (Supporting Information, Figure S1). Ti/Au (3/30 nm) electrodes were then deposited by plasma sputtering onto masked graphene samples as demonstrated in Figure 1a with robust ohmic contact (Supporting Information, Figure S3). Graphs in Figure 1a,b show two kinds of samples with different sizes for testing. The sample shown in Figure 1a was patterned with two electrodes and its area confined between the electrodes has a dimension of 1 × 1.5 ($W \times L$) cm^2 when mounted on a SiO_2/Si substrate and 2 × 12 cm^2 when on a PET substrate. Another sample in Figure 1b was patterned well-proportionally with nine electrodes along the length direction of the graphene on the SiO_2/Si substrate; the spacing between any two adjacent electrodes is uniformly 75 μm, except for the E0 that is aligned along the flow direction, and the width of each electrode is 2 mm. Silver epoxy and metal wires with insulating skin were used to connect the electrodes for electric measurement.

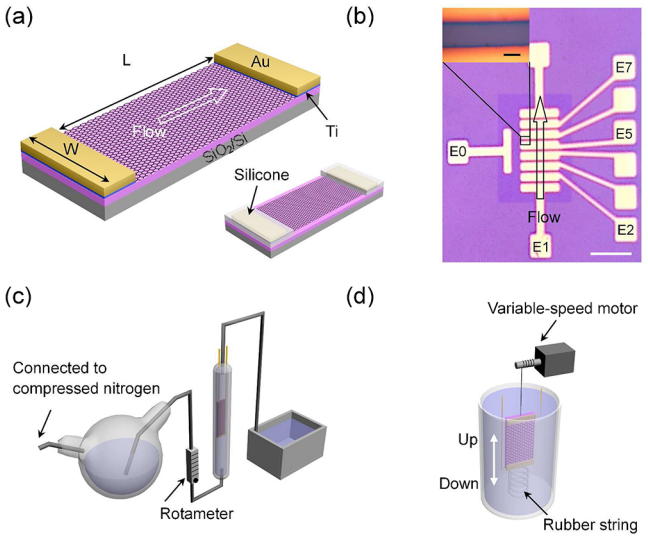

Figure 1. Prepared samples and designed experimental setups. (a) Schematic illustration of a two-terminal graphene sample mounted on a 300 nm SiO_2/Si (or PET for large samples) substrate. Ti/Au electrodes were patterned on the two ends of the graphene sample and protected by silicone to avoid exposing to the HCl solution (inset). The flow is along the length direction L of the sample as denoted by the white arrow. (b) Optical image of a graphene sample on the SiO_2/Si substrate with nine Ti/Au electrodes. Electrode E0 is along the flow direction and the remaining eight electrodes from E1 to E8 are equally spaced perpendicular to the flow direction. The up-left inset is a magnified view of the graphene region between two adjacent electrodes. Scale bar is 2 mm in (b) and 50 μm in the inset. (c,d) Schematic illustrations of typical experiment setups A and B, respectively. (c) Sample sets in a uniform pipe flow of the HCl solution driven by compressed nitrogen gas in a cylinder connected to the water container, and the pipe flow velocity is controlled by a rotameter. (d) Sample moves up and down in static HCl solution tank. The lower end of the sample is connected to the bottom of the container by an elastic string. The moving velocity of the sample is controlled by a motor.

Figure 1c,d depicts two kinds of experimental setups, A and B, used in our following measurements, respectively. The setup A is for the graphene samples immersed in flowing HCl water as illustrated in Figure 1c. For facile realization of a controllable uniform flow of HCl water through a 40 cm long pipe (2.4 cm in diameter), the HCl water is pressured upward through the pipe by the compressed nitrogen gas. The graphene sample is aligned parallel to the flow direction and placed at the center of the pipe, where the water flow is expected to be laminar for its low Reynolds number within the velocity range examined in our experiment. The velocity of the water flow is controlled by a rotameter valve and calculated by the readout of the rotameter and the cross-section area of the pipe. In contrast, the setup B is for the sample moving in static HCl water at a given velocity (see Figure 1d). The graphene sample is driven by a variable-speed motor to move up and down in the HCl water. The end of the sample is connected to the bottom of the water container through a elastic string to make sure that it follows the motor's operation for stabilizing the motion. The velocity of the sample is controlled by adjusting the motor. To minimize the influence of the motion of the connected wire on the measured voltage signal, a thin flexible wire was chosen here. If without specific statements, all the following tests are performed in the 0.6 M HCl water at room temperature. The voltage is measured in real time by a KEITHLEY 2010 multimeter.

First, we measured the electric response in few-layered graphene samples of 1 × 1.5 cm^2 in size to the HCl water flow as put into practice in the setup A, with electrodes being completely covered with silicone to prevent from interacting with the HCl water, as shown in the inset of Figure 1a. Note that the section of sample confined between the electrodes keeps exposed to the HCl water throughout the measurement. Figure 2a shows that there is no noticeable change in the voltage signals for all the graphene samples upon switching on the water flow at a velocity of 1.05 cm/s for 15−20 s and then turning it off. The voltage only fluctuates at its noise level, although the noise level is somewhat different in the monolayer, bi-, and trilayered graphene samples due to their different resistances. The resistances for the measured monolayer, bi-, and trilayered graphene samples are 2.12, 0.97, and 0.8 kΩ, respectively, the square root of which are proportional to the induced noise voltage according to the theory of Johnson−Nyquist noise. These results indicate that water flow over mono- and few-layered graphene samples connected between covered electrodes cannot induce measurable voltage, which is in sharp contrast to the previous results that a 30 × 16 μm^2 size graphene surface with exposed electrodes can generate a peak voltage ~25 mV at almost the same velocity of 1 cm/s. Similar results also exists in samples

dx.doi.org/10.1021/nl300636g | Nano Lett. 2012, 12, 1736−1741

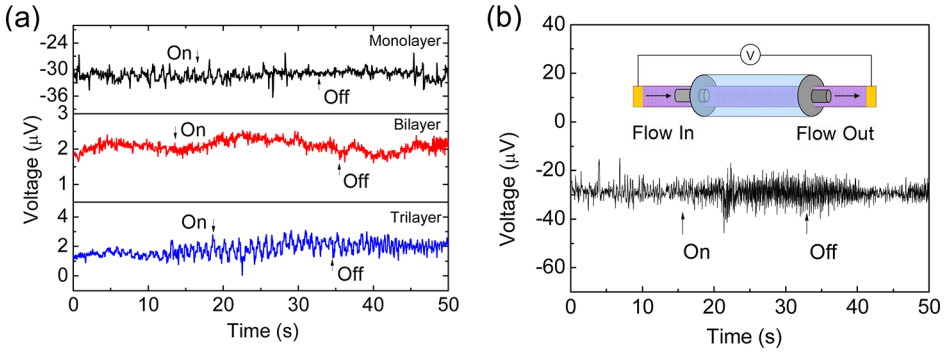

Figure 2. Voltage response of graphene sample to the uniform water flow in a pipe at v = 1.05 cm/s. The arrows mark where the flow is turned on and off. (a) The voltage signal produced in mono-, bi-, and trilayer graphene samples of 1 × 1.5 cm^2 in size with covered electrodes. (b) Voltage signal produced in a graphene sample (size: 2 × 12 cm^2) with the electrodes outside of the solution chamber. In this case, only the graphene middle section of 8 cm in length is immersed in the pipeline water with both the graphene ends and electrodes located outside of the pipe, see the inset. The flow direction is indicated by the arrows.

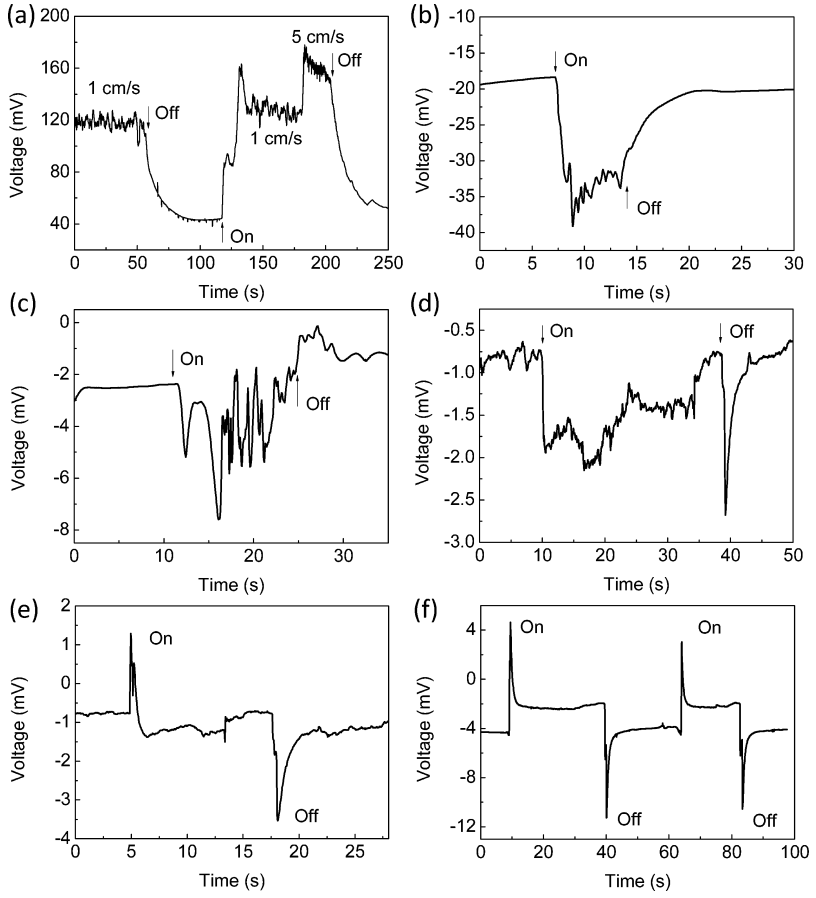

Figure 3. Evolution of the voltage induced by HCl water flow in a 1 × 1.5 cm^2 sample with exposed electrodes. On and Off in the figures mark the positions where the flow is switched on and off, respectively. (a) Voltage signal response in a newly prepared sample to the flowing HCl water. (b) Electric signal in the sample that was exposed in air for 24 min from the measurement in (a). In this measurement, the sample was reversed in orientation from that in (a). (c) Electric signal in the sample that was turned back in orientation to that in (a). (d–f) The voltage signals measured after the graphene sheet is further exposed in air for 19 h: (d) the initial signal and (e,f) the signals after a time interval of 3 and 6 min, respectively. The flow velocity is uniformly set to 1 cm/s for the results shown in (a–f).

with covered electrodes made of different materials, such as silver epoxy (Supporting Information, Figure S4). More extensively, the same negligible signals are obtained by moving the same-sized samples immersed in the HCl water at a velocity of 4.2 cm/s using the setup B and still occur even in a remarkably larger sample with a size up to 2 × 12 cm^2 (Supporting Information, Figure S5).

To be more convinced, we further performed experiments by a specific setup as shown by the inset of Figure 2b: the middle section (8 cm long) of a graphene sample of 2 × 12 cm^2 in size on the PET substrate is encapsulated in a pipe, leaving the two graphene ends outside the pipe to connect the electrodes out of the water. As can be envisioned from the above discussion, there is no measurable electric response when the same HCl

dx.doi.org/10.1021/nl300636g | Nano Lett. 2012, 12, 1736–1741

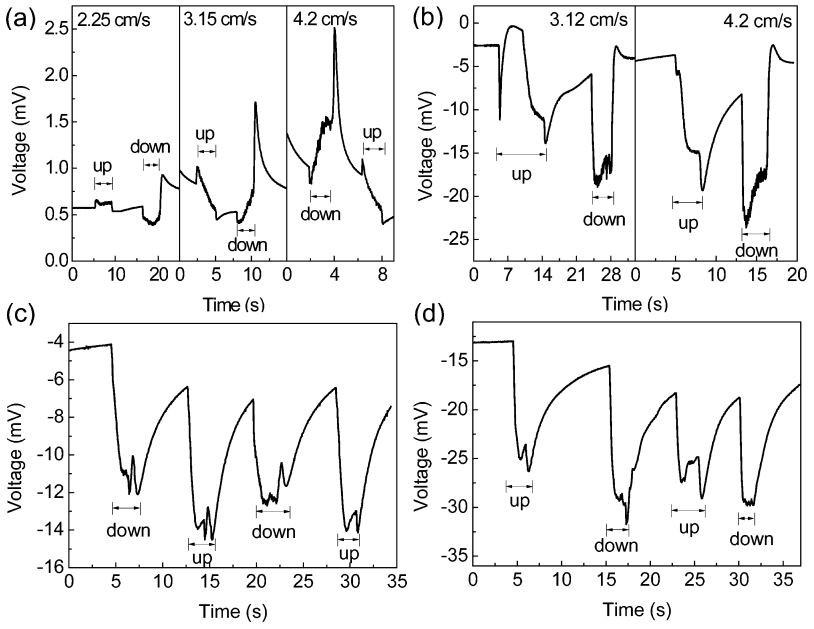

Figure 4. Voltages produced by the sample with exposed nine-electrodes moving up and down in static 0.6 M HCl solution in the setup B shown by Figure 1d. The signals marked by up and down are induced by moving the sample up and down, respectively. The voltage measured between the electrodes (a) E1 and E2, (b) E1 and E7 at different velocities. (c) The voltage signal between electrodes E0 and E5 at velocity of 2.25 cm/s. (d) The voltage between electrodes E0 and E5 at 2.25 cm/s when the graphene sample is removed and instead a 15 kΩ load resistor is connected in the external circuit outside the HCl water.

water flow was switched on and off (Figure 2b). Therefore, we are convinced that immersed graphene itself can not harvest the flow energy in the ionic water.

To explore the role of the exposed electrodes in creating the flow-induced voltage, we then conducted experiments on graphene samples with the Ti/Au electrodes exposed to the flowing water. In these tests, only the wire connection sites were covered by silicone. Figure 3 shows the real-time flow-induced voltage signals in a 1 × 1.5 cm^2 graphene sample as shown in Figure 1a by the setup A. The size of each electrode is 1 × 0.5 cm^2 and the area ratio of graphene to the two exposed electrodes is 1.5. First, when switching on a flow with velocity v = 1 cm/s, the voltage reaches and stabilizes around 120 mV as shown in Figure 3a. Once the flow is switched off, the voltage drops to a resting voltage ∼43 mV in duration of about 30 s. With switching the flow on again, the voltage rises quickly and reaches about 125 mV, which can be further enlarged to 175 mV by increasing the flow velocity to 5 cm/s at which the flow-induced voltage cannot stabilize but decays fast at the fixed flow velocity. The voltage dropped gradually to the resting voltage again when switching the flow off. This retarded dropping process suggests that the flow-induced voltage is not directly related to the water flow.

However, this flow-induced voltage is extremely unstable via repeatedly exposing the samples to the environments. Figure 3b–f shows the evolution of the flow-induced voltage at different stages. Figure 3b shows the results measured after the sample was exposed for 24 min to air environment and then reversely put back to the pipe. Both the resting voltage and flow-induced signal at velocity v = 1 cm/s are reversed to be negative with amplitudes reduced to ∼18 and ∼35 mV, respectively. After turning the sample back to its original orientation and put back to the testing pipe again, the voltage signals remain in negative, as shown by Figure 3c. Nevertheless, there is no stable response to the water flow any longer, and the resting voltage drops to 0 to −2 mV. After the sample was placed in air environment again for 19 h, the voltage signals initially become two times lower and remain highly unstable as shown in Figure 3d. So the induced voltage is very sensitive to exposing the sample to the environment. Once the sample is fully immersed in the flowing HCl water for several minutes, the signal gradually evolves into a stable voltage signal, as evidenced by the change in electric signal measured in the first 3 min (Figure 3e) to that measured in later 6 min (Figure 3f). Especially, the signal in Figure 3f shows a stable resting potential at around −4 mV. In this case, the voltage increases sharply to 4 mV when the flow is switched on and then swiftly stabilizes at −2 mV. Once the flow is switched off, this voltage will be sharply decreased to a negative peak of −10 mV and then quickly return to the resting potential. This process can be repeated to form a stable, regular signal by continuously switching the flow on and off. We attribute the stability of the signal to blunting of the electrode surface via a substantial interaction with the environment, so that the local potential of the electrodes is no longer sensitive to the local environment surrounding the electrodes, expect for the moment of switching the flow on or off. Finally, if the blunted electrodes on the graphene sample are covered by silicone, no measurable voltage response to the water flow can be obtained any more (Supporting Information, Figure S6).

To further explore the effect of relative positions of the electrodes and space between the electrodes, we conducted experiments with the nine-electrode samples moving at various velocities in the 0.6 M HCl water using the setup B. The electrodes are exposed to the water but the connection sites are sealed from the liquid by silicone. Some typical results are presented in Figure 4. The measured voltage between electrodes E1 and E2 is shown in Figure 4a. Although the voltage response increases with increasing velocity of the sample moving up and down in the water, the signal does not

dx.doi.org/10.1021/nl300636g | *Nano Lett.* 2012, 12, 1736–1741

form a regular square wave to the up−down motion at higher velocities. It is interesting that the measured voltage signals between two further spaced electrodes E1 and E7 shown in Figure 4b are significantly stronger than that produced between the electrodes E1 and E2 shown in Figure 4a. There are two possible reasons accounting for this electrode spacing effect. One is as explained by Dhiman et al.[1] that flow-induced voltage in graphene can be amplified with increasing graphene size, but this has been denied by our above experiments on the macroscopic graphene samples with the electrode−solution interaction excluded by covering electrodes or locating electrodes out of the solution as shown in Figure 2. Another one is that graphene should behave as a load connected between the electrodes, rather than the electricity producer. The larger load resistance connected between electrodes E1 and E7 thus leads to a higher voltage. Even between the electrodes E0 and E5, which are aligned perpendicular to the flow direction asymmetrically, the induced voltage can reach tens of millivolts when the sample is moving up and down at a velocity of 2.25 cm/s in the HCl water (see Figure 4c). However, the sign of the induced voltage is unchanged upon changing the moving direction of the sample. This is difficult to be explained by flow-driven transfer of charge carriers in graphene as conceived previously in literatures. To further confirm the role of electrodes in the measured voltage responses, we repeated the same measurement by connecting a 15 kohm load made of a carbon film resistor between electrodes E0 and E5 in the external circuit outside the HCl water, but with the graphene between the electrodes removed. The induced voltage between the electrodes is shown in Figure 4d. Surprisingly, the response is nearly the same as in the measurements with the graphene sample in place, except for a higher resting voltage. These results affirm that the observed flow-induced voltage up to tens of millivolts in the graphene samples with exposed electrodes is mainly attributed to the electrode−solution interaction, while the graphene more acts as a load to transport the charge carriers between the exposed electrodes.

To get deeper insight into the absence of flow-induced voltages in immersed graphene itself, we perform density-functional theory calculations on the interaction of a graphene sheet with the ionic species present in the HCl solution, as implemented with the VASP code[17,18] (see the details in Supporting Information). In the HCl solution, there are mainly two kinds of ions, the hydronium cations and hydrated Cl^- anions. Our results show that the hydronium cation can form a covalent bond with the graphene sheet with a binding energy up to 2.8 eV, while the hydrated Cl^- anion is repulsive to graphene because of its negative adsorption energy. This is reflected by the structure deformation in the graphene sheet with an adsorbed hydronium cation, as shown in Figure 5a, which is in contrast to the perfect graphene plane adsorbed with a hydrated Cl^- anion (Figure 5b). Therefore, once the graphene sheet is immersed in the HCl solution, the hydronium cation will adsorb onto the graphene sheet but the Cl^- anion will be repulsed from it due to their different behaviors in charge exchange with graphene. This is in sharp contrast to the empirical force-field results reported by Dhiman et al.:[1] the Cl^- anion can adsorb, desorb, and hop on the graphene while hydronium cation has a weak interaction with the graphene. This discrepancy is attributed to that the force-field molecule dynamics treats the hydronium cation as an rigid charged ball and fails to capture the significant charge exchange.

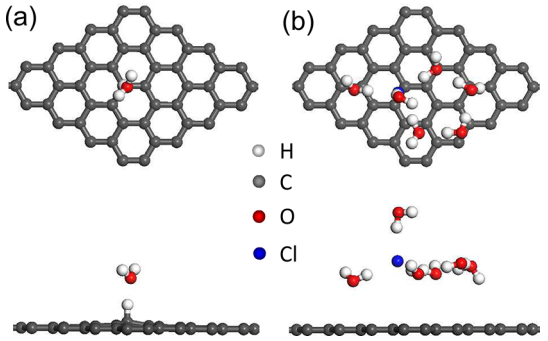

Figure 5. Atomic structure for the (a) hydronium cation and (b) hydrated Cl^- anion adsorbed on a 5 × 5 unit monolayer graphene. Top and down panels show the top and side views of the atomic motifs, respectively.

Therefore, the force-field molecule dynamics simulation is incompetent to study the interaction of graphene with charged ions in the ionic solutions. Our atomistic study thus denies the coupling of free graphene carries with the flowing ions as the major mechanism for the flow-induced voltage and further convinces the importance of the electrode−solution interaction in producing the voltage.

We also find that for a graphene sheet immersed in other flowing salt waters, the electrode−solution interaction remains the driving source of the induced voltage. For example, the flow-induced voltage for graphene in NaCl solution remains at the noise level when covering the electrodes but can increase to 0.04 mV when exposing the electrodes to the solution (Supporting Information, Figure S7). The induced voltage here is lower than that for the HCl solution, just because the electrode−solution interaction is much milder in the NaCl solution. Our further extensive calculations show that the cations in a series of ionic waters always dominate the interaction with graphene over the anions. We find that the interaction of cations is even enhanced with CNTs, that is, a curved graphene surface, especially for the H_3O^+ cation that shows stronger covalent adsorption (Supporting Information, Figure S8). However, our measurements show that a piece of CNT film immersed in the flowing HCl water can generate a voltage of several millivolts with the signal sign unchanged when reversing the flow directions, although the electrodes are covered (Supporting Information, Figure S9). Here, the CNT edges should be ruled out as the source for the induced voltage, since our measurements have identified that the exposed graphene edges have negligible contribution to the flow-induced voltage. The possible reason is that the CNT film contains a lot of metal catalyst particles during the growth process,[19,20] which can interact with solution to produce measurable voltages. A recent experiment[4] shows that a single-walled CNT film aligned perpendicularly to the flow of KCl solution can produce voltage up to tens of microvolts but still with exposed electrodes. This result is consistent with our measured signal between the electrodes E0 and E5 as shown in Figure 4c, thus further supporting the role of metal−solution interaction in producing the voltage.

All our above experimental and theoretical results indicate that flow-induced voltage should not be attributed to the coupling of charge carrier in graphene with the flowing ions in solutions as well as the electron dragging by phonon wind resulting from liquid molecules. In the HCl water, hydronium cations bind strongly to the graphene sheet through forming

dx.doi.org/10.1021/nl300636g | Nano Lett. 2012, 12, 1736−1741

covalent bonds. No measurable voltage can be detected in mono- to few-layered graphene samples with covered electrodes immersed in the flowing HCl water. In the previously reported flow-induced voltage in ref 1, the graphene mainly behaves as a load connected between the electrodes, rather than the electricity producer. Instead, the electrode−solution interaction play a central role in producing the observed voltage: as the sample is immersed in the HCl water, an electrochemical potential is introduced for the electrodes; the water flow changes the electrostatic potential,[21] breaks the electrochemical balance, and introduces potential differences between the electrodes. This voltage is unstable and very sensitive to the change in local environment surrounding the electrodes. Once the electrodes are prevented to interact with the ionic waters, the voltage immediately disappears as the electrode−solution interaction is cut off. The results not only reveal the real picture of how the energy is harvested by the small graphene region surrounded by large metallic electrodes in ref 1 but also call for a turning point on researches of flow-induced voltage by carbon nanomaterials.

■ ASSOCIATED CONTENT

Ⓢ Supporting Information

Method of the theoretical calculations, Raman spectroscopy of few-layered graphene samples, atomic force microscopy topography of monolayer graphene sheet, current−voltage curve of the sample, voltage response of graphene sample with covered silver epoxy electrodes and graphene sample with size of 2×12 cm^2, induced voltage after the electrodes are covered, flow-induced voltage in the 0.6 M NaCl solution, atomic structure for the (10,0) and (5,5) CNTs with adsorbed hydronium cation, and flow-induced voltage in CNT thin films are collected. This material is available free of charge via the Internet at http://pubs.acs.org.

■ AUTHOR INFORMATION

Corresponding Author

*E-mail: wlguo@nuaa.edu.cn.

Notes

The authors declare no competing financial interest.

■ ACKNOWLEDGMENTS

This work was supported by 973 program (2012CB933403), the National and Jiangsu NSF (10732040, 91023026, 11172124, BK2008042) of China. We thank Professors Qingwen Li for providing the CNT samples.

■ REFERENCES

(1) Dhiman, P.; Yavari, F.; Mi, X.; Gullapalli, H.; Shi, Y.; Ajayan, P. M.; Koratkar, N. *Nano Lett.* **2011**, *11*, 3123−3127.
(2) Ghosh, S.; Sood, A. K.; Kumar, N. *Science* **2003**, *299*, 1042−1044.
(3) Liu, J.; Dai, L.; Baur, J. W. *J. Appl. Phys.* **2007**, *101*, 064312.
(4) Lee, S. H.; Kim, D.; Kim, S.; Han, C.-S. *Appl. Phys. Lett.* **2011**, *99*, 104103.
(5) Král, P.; Shapiro, M. *Phys. Rev. Lett.* **2001**, *86*, 131−134.
(6) Cohen, A. E. *Science* **2003**, *300*, 1235−1236.
(7) Persson, B. N. J.; Tartaglino, U.; Tosatti, E.; Ueba, H. *Phys. Rev. B* **2004**, *69*, 235410.
(8) Yuan, Q. Z.; Zhao, Y.-P. *J. Am. Chem. Soc.* **2009**, *131*, 6374−6376.
(9) Ghosh, S.; Sood, A. K.; Ramaswamy, S.; Kumar, N. *Phys. Rev. B* **2004**, *70*, 205423.
(10) Li, X. S.; Cai, W. W.; An, J.; Kim, S.; Nah, J.; Yang, D. X.; Piner, R.; Velamakanni, A.; Jung, I.; Tutuc, E.; Banerjee, S. K.; Colombo, L.; Ruoff, R. S. *Science* **2009**, *324*, 1312−1314.
(11) Li, X. S.; Magnuson, C. W.; Venugopal, A.; An, J.; Suk, J. W.; Han, B. Y.; Borysiak, M.; Cai, W. W.; Velamakanni, A.; Zhu, Y. W.; Fu, L. F.; Vogel, E. M.; Voelkl, E.; Colombo, L.; Ruoff, R. S. *Nano Lett.* **2010**, *10*, 4328−4334.
(12) Li, X. S.; Zhu, Y. W.; Cai, W. W.; Borysiak, M.; Han, B. Y.; Chen, D.; Piner, R. D.; Colombo, L.; Ruoff, R. S. *Nano Lett.* **2009**, *9*, 4359−4363.
(13) Suk, J. W.; Kitt, A.; Magnuson, C. W.; Hao, Y.; Ahmed, S.; An, J.; Swan, A. K.; Goldberg, B. B.; Ruoff, R. S. *ACS Nano* **2011**, *5*, 6916−6924.
(14) Liang, X. L.; Sperling, B. A.; Calizo, I.; Cheng, G. J.; Hacker, C. A.; Zhang, Q.; Obeng, Y.; Yan, K.; Peng, H. L.; Li, Q. L.; Zhu, X. X.; Yuan, H.; Hight Walker, A. R.; Liu, Z. F.; Peng, L. M.; Richter, C. A. *ACS Nano* **2011**, *5*, 9144−9153.
(15) Reina, A.; Jia, X. T.; Ho, J.; Nezich, D.; Son, H.; Bulovic, V.; Dresselhaus, M. S.; Kong, J. *Nano Lett.* **2008**, *9*, 30−35.
(16) Ferrari, A. C.; Meyer, J. C.; Scardaci, V.; Casiraghi, C.; Lazzeri, M.; Mauri, F.; Piscanec, S.; Jiang, D.; Novoselov, K. S.; Roth, S.; Geim, A. K. *Phys. Rev. Lett.* **2006**, *97*, 187401.
(17) Blöchl, P. E. *Phys. Rev. B* **1994**, *50*, 17953−17979.
(18) Kresse, G.; Furthmüller, J. *Phys. Rev. B* **1996**, *54*, 11169−11186.
(19) Hata, K.; Futaba, D. N.; Mizuno, K.; Namai, T.; Yumura, M.; Iijima, S. *Science* **2004**, *306*, 1362−1364.
(20) Liu, K.; Sun, Y. H.; Chen, L.; Feng, C.; Feng, X. F.; Jiang, K. L.; Zhao, Y. G.; Fan, S. S. *Nano Lett.* **2008**, *8*, 700−705.
(21) Bourlon, B.; Wong, J.; Miko, C.; Forro, L.; Bockrath, M. *Nat. Nanotechnol.* **2007**, *2*, 104−107.